PROCEEDINGS OF SCIENCE

The Steady-State Multi-TeV Diffuse Gamma-Ray Emission Predicted with GALPROP and Prospects for the Cherenkov Telescope Array

P. D. Marinos,[a,*] **G. P. Rowell,**[a] **T. A. Porter**[b] **and G. Jóhannesson**[c]

[a] *School of Physical Sciences, University of Adelaide, Adelaide, South Australia 5000, Australia*

[b] *W. W. Hansen Experimental Physics Laboratory and Kavli Institute for Particle Astrophysics and Cosmology, Stanford University, Stanford, CA 94305, USA*

[c] *Science Institute, University of Iceland, IS-107 Reykjavik, Iceland*

E-mail: peter.marinos@adelaide.edu.au, gavin.rowell@adelaide.edu.au, tporter@stanford.edu, gudlaugu@hi.is

Multi-TeV cosmic rays (CRs) form a "sea" of particles within the Galactic plane, resulting in a diffuse gamma-ray emission visible across a broad energy range. The Fermi Large Area Telescope has measured these gamma-ray emissions at GeV energies with high statistics, and recent results from H.E.S.S., HAWC, LHAASO, and the Tibet Air-shower Array show that the diffuse gamma-ray emission extends into the TeV and PeV energy regimes. The emissions observed at GeV and TeV energies are connected by the common origin of the CR particles injected by the sources; however, the CR sources, their energy dependence, and the relative composition of the CRs, are not well understood. In this contribution we use the 3D simulation software GALPROP to model CR diffusion across the Galaxy. Using a grid of steady-state models we compute the first quantitative measure of the variation in the diffuse gamma-ray flux that arises from uncertainties in the CR source positions, the interstellar radiation field, and the Galactic magnetic field. We provide the first longitudinal profiles of the modelled gamma-ray emission up to 100 TeV from GALPROP along the Galactic plane and compare the model predictions to the H.E.S.S. Galactic plane survey (HGPS) after carefully subtracting emission from catalogued TeV gamma-ray sources. We found that the GALPROP model predictions agree with the lower estimates for the HGPS source-subtracted diffuse flux. Our results show that the next generation Cherenkov telescope array (CTA) should be able to observe the diffuse emission if appropriate measures are taken to subtract background emission.

38th International Cosmic Ray Conference (ICRC2023)
26 July - 3 August, 2023
Nagoya, Japan

*Speaker

PoS(ICRC2023)876

1. Introduction

Cosmic ray particles are injected by sources, propagating throughout the Galaxy over millions of years. This process results in a 'sea' of CRs that produce broadband all-sky emissions due to energy losses with the other components of the diffuse ISM: the interstellar gas, the interstellar radiation field (ISRF), and the Galactic magnetic field (GMF). The diffuse emissions by the CRs encode critical information on the CR sources, how CRs are injected into the ISM and their propagation history, as well as the spatial distributions of the other ISM components. Observations of their non-thermal emissions can be used to provide essential insights for understanding how the CRs are accelerated up to the highest energies within the Galaxy.

At GeV γ-ray energies the sky is dominated by the emissions produced by the CR sea throughout the Milky Way (MW), which have been measured and studied extensively with the *Fermi*–LAT [1]. For the TeV energy range, the emissions about source regions are brighter than the diffuse emission. The recent release of the H.E.S.S. Galactic plane survey [2] shows localised, extended regions embedded in lower-intensity, broadly distributed emissions

The VHE diffuse emission is currently observed with low significance by H.E.S.S. [3]. There is a connection between the GeV and TeV energy ranges, but the energy dependence of the mixture of emissions from the general ISM (true 'diffuse'), those emanating from the relatively nearby interstellar space about the sources, and the sources themselves, is not well understood. Accurately determining the relative contributions will be essential for the next generation of facilities that will have a significantly enhanced sensitivity. An example is the Cherenkov Telescope Array [CTA; 4], which is currently under construction. The lower flux levels that CTA will reach, and its much larger field of view, will make it extremely sensitive to the details of the diffuse emissions. CTA will also detect hundreds of new γ-ray sources. Consequently, source confusion, together with the other emissions, will likely be a significant issue that will need to be addressed.

2. GALPROP

For our modelling we use the latest release (v57) of the Galprop framework [5, 6]. For an assumed propagation phenomenology, the critical inputs for a Galprop run are the CR source density distribution, the ISM gas, the ISRF, and the GMF. We fix the interstellar gas model and make predictions for combinations of the interstellar radiation and magnetic field distributions over a range of CR source density distributions. A full description of the 3D models used here is given in [7].

2.1 The CR Source Distributions

We construct a set of synthetic distributions comprised of a disc-like component and a spiral arm component to investigate the effect of the 3D source distribution on the VHE γ-ray emissions. The spiral arms have the geometry of those for the R12 ISRF model (see below), but with equal weighting for their normalisations. Our CR source distributions start with a purely disc-like distribution (that we term SA0), and increase with relative contribution by the spiral arms until the distribution is purely due to the spiral arms (termed SA100). Consequently, we have the SA0, SA25, SA50, SA75, and SA100 distributions corresponding to 0, 25, 50, 75, and 100%, respectively, for

the source luminosity contained in the spiral arms, with the remaining source luminosity in the disc-like component. The primary CR source spectra and other parameters are determined for each model by the optimisation procedure described in [7].

2.2 The Interstellar Radiation and Magnetic Fields

The CR electrons and positrons lose energy via Compton and synchrotron interactions with the interstellar radiation and magnetic fields. Into the VHE range, these processes strongly influence the CR spectral intensities and correspondingly affect the intensity distribution for the γ rays. Because there is still uncertainty for the ISRF and GMF distributions, we employ representative models that are available within the GALPROP framework.

The ISRF encompasses the electromagnetic radiation within the Galaxy, including emission from stars, infrared light from interstellar dust radiating heat, and the cosmic microwave background (CMB). The state-of-the-art 3D ISRF models are based on spatially smooth stellar and dust models. They have designations R12 and F98 that correspond to the respective references supplying the stellar/dust distributions [8, 9]. Both reproduce the data, but neither is an overall best match. The R12 model provides better correspondence toward the spiral arm tangents, but does not display the asymmetry associated with the bar, and the stellar disc scale length is incompatible with the near-IR profiles. Meanwhile, the F98 model has the disc scale-length in better agreement with the near-IR data, incorporates the bulge/bar asymmetry, but has none of the structure associated with the spiral arms.

The GMF consists of the large-scale regular and small-scale random components that are about equal in intensity. Here we use the bisymmetric spiral GMF model from [10], that we refer to as PBSS, as a representative model with a spiral structure. We also employ the GALPROP axisymmetric exponential distribution [GASE; 11]. The GASE distribution is a simple, exponentially decreasing field in both Galactocentric radius and height above the plane, and does not include the spiral arms.

2.3 Parameter Optimisation

To ensure that each combination of inputs reproduces the local CR spectra, the propagation parameters are optimised for each CR source distribution. We follow the procedure outlined in [7] (and references therein). For each of the source distributions, an initial optimisation of the propagation models is made by fitting to the observed CR spectra from AMS-02 and *Voyager 1* in the GeV energy range, where the CR sea is the dominant source of CRs. This procedure is performed for the CR species: Be, B, C, O, Mg, Ne, and Si. These are kept fixed, and the injection spectra for electrons, protons, and He are tuned together. This process is performed iteratively until convergence. For the multi-TeV electrons, local measurements cannot be used to constrain the injection spectrum due to the short (<1 kpc) travel distances. As electrons are known to be accelerated in the MW up to PeV energies by PWNe, no artificial cut off is applied to the CR electron injection spectrum for our models. The parameters that vary with the source distributions are given in [7, Table 1].

2.4 Interstellar Emissions Modelling Predictions

The γ-ray intensity maps at the solar system location are obtained by line-of-sight (LOS) integration of the γ-ray emissivities for the standard processes (π^0-decay, IC scattering), where the

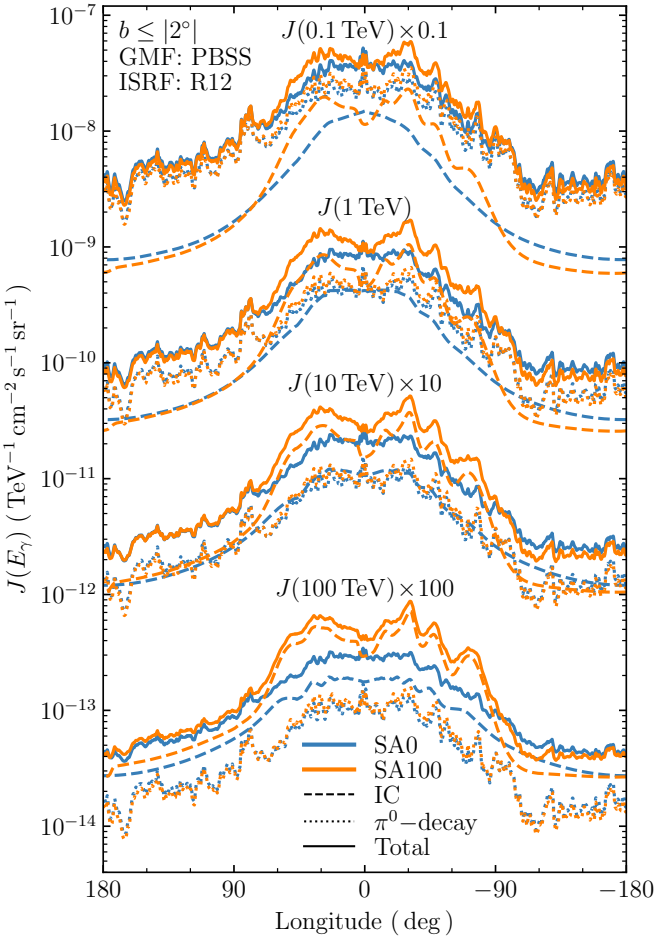

Figure 1: Longitude profile for $b \leq |2^\circ|$ along the Galactic plane for various energies using the R12 ISRF and the PBSS GMF distributions. The source distributions shown are SA0 (blue) and SA100 (orange), and the emission types shown are IC (dashed), π^0-decay (dotted), and the total flux (solid). The profiles have been multiplied by the given factors to increase contrast.

emissivities are determined for a logarithmic grid from 1 GeV to 100 TeV using five bins per decade spacing. We use a HEALPix [12] order 9 isopixelisation for the skymap generation. The pixel size is 6.9′, which is similar to the point-spread function of H.E.S.S. (4.8′). The $\gamma\gamma \rightarrow e^{\pm}$ attenuation that affects the γ-ray intensities for $\gtrsim$10 TeV is included in the LOS integration, where the optical depth calculation includes the directionality of the ISRF [13, 14].

Figure 1 shows the longitudinal profile of the IC and π^0-decay emission for the various source distributions for energy levels between 0.1 TeV and 100 TeV. The π^0-decay dominates the γ-ray emission for all longitudes for the energies $E < 1$ TeV. Meanwhile, the IC emission becomes dominant for $\gtrsim$10 TeV energies. Because the energy losses are much faster for the electrons, its contribution to the profiles is much more sensitive to changes in the source distribution over most of the Galactic plane. As the majority of the spiral arms are located between Earth and the GC, with one of the arms located in close proximity to the Earth, we see that for a larger fraction of CRs being injected into the spiral arms (e.g. SA100) the IC component becomes more intense for the central

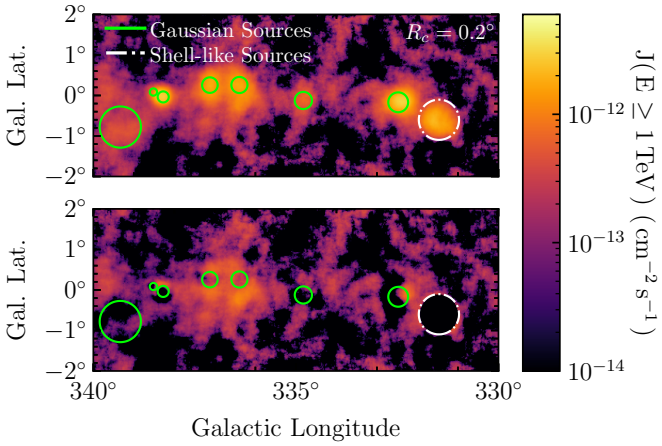

Figure 2: HGPS flux in cm^{-2} s^{-1} for Galactic longitudes $340° \leq l \leq 320°$ for the $R_c = 0.2°$ map, before (top panel) and after (bottom panel) sources are masked from the image. Gaussian sources are shown with a solid green circle and shell-like sources are shown with white dash-dot circles.

region (i.e. $l \leq |50°|$). The IC emission is also boosted along the spiral arm tangents located at $l \approx |20°|$. For the negative longitudes between the anti-centre and perpendicular to the GC, i.e. for $-90° < l < -180°$, the IC emission decreases with an increasing fraction of CR injection in the spiral arms, and the difference between the source density distributions increases with increasing energy.

Across the entire plane for all source distributions the IC emission dominates the γ-ray emission at 100 TeV. It is not a surprise that the spiral structure in the source density distributions including arms is evident in the profiles. However, at these energies there also appears to be structure for the SA0 density distribution IC profile similar to those models including arms that is not apparent at lower energies. Because of the KN suppression for the optical and IR components of the ISRF, the only photon field is the (uniform) CMB for IC processes. The energy density of the GMF varies, but is much higher than that for the CMB about the spiral arms, and hence determines the energy loss time scale affecting the electron distribution. The observed structure in the 100 TeV IC profile for the SA0 distribution is therefore entirely due to that encoded in the PBSS GMF distribution, with its influence imprinted on the electron energy density.

3. HGPS

Our analysis of the HGPS uses the survey sky map with an integration/containment radius of $R_c = 0.2°$ such that we are as sensitive as possible to the TeV diffuse γ-ray emission. We then use a sliding window method with parameters suitably optimised to reveal the longitudinal structure of the diffuse emission (see [7]).

The sliding window is applied after the masking of known catalogued sources. The HGPS catalogued 78 sources in TeV γ rays. The Galactic centre and shell-like morphological structures are excluded from the analysis. The remaining sources are modelled as one or more Gaussians, with their surface brightness being subtracted from the map. A demonstration of the source masking procedure can be seen in Figure 2.

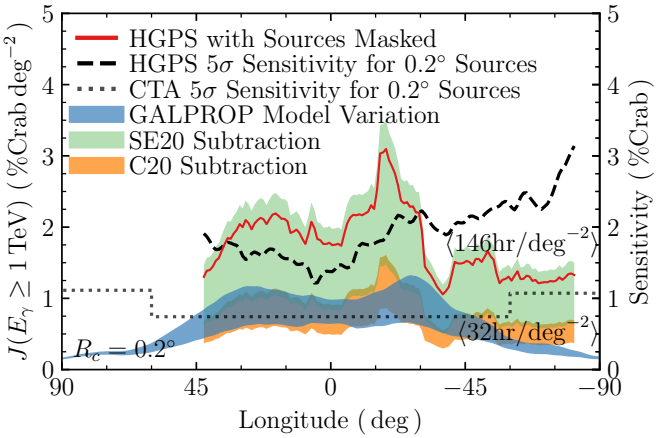

Figure 3: Longitudinal profiles integrated above 1 TeV for the GALPROP variation (blue) and the HGPS after catalogued sources are subtracted (solid red), shown after the sliding window has been applied for a containment radius of $R_c = 0.2°$ in units of %Crab deg^{-2}. Also shown are the results after subtracting the unresolved sources, with the estimates of the unresolved sources calculated from the estimates given by [15] (SE20; green) and [16] (C20; orange). The 5σ sensitivity is shown for the HGPS (dashed black) and CTA GPS (dotted black) when using a containment radius of $R_c = 0.2°$, both of which are shown in units of %Crab. Averaging windows were applied to both the HGPS and the GALPROP profiles, and have a width of $\Delta w = 15°$ and height of $\Delta h = 2.5°$, centred at a latitude of $b_0 = -0.25°$ and spaced $\Delta s = 1°$ apart.

It is also necessary to account for the unresolved sources, i.e. the ensemble of γ-ray sources below the detection threshold of H.E.S.S.. Although they are not individually resolved, these unresolved sources still contribute to the total observed Galactic emission, providing an extended low surface brightness contribution to the observed flux. As they are not part of the truly diffuse emission, their contribution must be subtracted. We use estimates for the unresolved source component from [15] (SE20) and [16] (C20) who give relative contributions to the HGPS of 13%–32% and 60%, respectively. We combine them with the systematic uncertainty in the H.E.S.S. fluxes to provide lower and upper limits for the diffuse γ-ray emission.

Figure 3 shows the source-subtracted flux obtained with our method, together with the bounding estimates employing the different unresolved source contributions. This is shown together with the longitudinal profile of the HGPS sensitivity in units of %Crab, where we use the definition $J_{\rm Crab}(E \geq 1\,{\rm TeV}) = 2.26 \times 10^{-11}\,{\rm cm}^{-2}\,{\rm s}^{-1}$ [17].

4. Discussion

We apply the same sliding window procedure to the GALPROP predictions over our model grid to enable a comparison with the HGPS diffuse flux estimates. Our GALPROP results were converted into units of %Crab deg^{-2} to allow comparisons to the HGPS sensitivity, which is given in units of %Crab. The GALPROP predictions are shown alongside the HGPS estimates after accounting for the γ-ray sources in Figure 3.

We can see that CTA-South should be able to detect the TeV diffuse γ-ray emission to the 5σ level given our most conservative estimates of the diffuse γ-ray emission predicted in this paper for

the central 80° of longitude ($|l| \leq 40°$). As has already been seen with the sensitive Fermi-LAT data at lower energies, separating individual source characteristics from the large-scale diffuse emission will require accurate models of the diffuse emission. These models will be essential for resolving and detecting faint, extended TeV emissions such as those such as those expected from PWN haloes, and for probing complex morphological structures of TeV sources. This will potentially allow the identification of currently unidentified sources in the HGPS and other current and future observations, such as those from CTA.

Acknowledgments

This research was supported by an Australian Government Research Training Program Scholarship, as well as student travel grants from both the Astronomical Society of Australia and the Australian Institute of Physics. GALPROP development is partially funded via NASA grants NNX17AB48G, 80NSSC22K0718, and 80NSSC22K0477. Some of the results have been derived using the `HEALPix` [12] and `Astropy` [18, 19] packages. This work was supported with supercomputing resources provided by the Phoenix HPC service at the University of Adelaide, and we want to thank Dr. F. Voisin in particular for his many hours spent configuring the HPC service to work efficiently with GALPROP.

References

[1] M. Ackermann, M. Ajello, W.B. Atwood, L. Baldini, J. Ballet, G. Barbiellini et al., *Fermi-lat observations of the diffuse γ-ray emission: Implications for cosmic rays and the interstellar medium*, *ApJ* **750** (2012) 3.

[2] H. Abdalla, A. Abramowski, F. Aharonian, F. Ait Benkhali, E.O. Angüner, M. Arakawa et al., *The H.E.S.S. galactic plane survey*, *A&A* **612** (2018) A1.

[3] A. Abramowski, F. Aharonian, F. Ait Benkhali, A.G. Akhperjanian, E.O. Angüner, M. Backes et al., *Diffuse galactic gamma-ray emission with h.e.s.s.*, *PhRvD* **90** (2014) 122007.

[4] CTA Consortium, B.S. Acharya, I. Agudo, I. Al Samarai, R. Alfaro, J. Alfaro et al., *Science with the Cherenkov Telescope Array*, World Scientific Publishing Company, Singapore (2019), 10.1142/10986.

[5] A.W. Strong and I.V. Moskalenko, *Propagation of Cosmic-Ray Nucleons in the Galaxy*, *ApJ* **509** (1998) 212 [astro-ph/9807150].

[6] I.V. Moskalenko and A.W. Strong, *Production and Propagation of Cosmic-Ray Positrons and Electrons*, *ApJ* **493** (1998) 694 [astro-ph/9710124].

[7] P.D. Marinos, G.P. Rowell, T.A. Porter and G. Jóhannesson, *The Steady-State Multi-TeV Diffuse Gamma-Ray Emission Predicted with GALPROP and Prospects for the Cherenkov Telescope Array*, *MNRAS* **518** (2023) 5036 [2211.01619].

[8] T.P. Robitaille, E. Churchwell, R.A. Benjamin, B.A. Whitney, K. Wood, B.L. Babler et al., *A self-consistent model of galactic stellar and dust infrared emission and the abundance of polycyclic aromatic hydrocarbons*, *A&A* **545** (2012) A39.

[9] H.T. Freudenreich, *A cobe model of the galactic bar and disk*, *ApJ* **492** (1998) 495.

[10] M.S. Pshirkov, P.G. Tinyakov, P.P. Kronberg and K.J. Newton-McGee, *Deriving the global structure of the galactic magnetic field from faraday rotation measures of extragalactic sources*, *ApJ* **738** (2011) 192.

[11] A.W. Strong, I.V. Moskalenko and O. Reimer, *Diffuse Continuum Gamma Rays from the Galaxy*, *ApJ* **537** (2000) 763 [astro-ph/9811296].

[12] K.M. Górski, E. Hivon, A.J. Banday, B.D. Wandelt, F.K. Hansen, M. Reinecke et al., *HEALPix: A Framework for High-Resolution Discretization and Fast Analysis of Data Distributed on the Sphere*, *ApJ* **622** (2005) 759 [arXiv: astro-ph/0409513].

[13] I.V. Moskalenko, T.A. Porter and A.W. Strong, *Attenuation of Very High Energy Gamma Rays by the Milky Way Interstellar Radiation Field*, *ApJL* **640** (2006) L155 [arXiv: astro-ph/0511149].

[14] T.A. Porter, G.P. Rowell, G. Jóhannesson and I.V. Moskalenko, *Galactic PeVatrons and helping to find them: Effects of galactic absorption on the observed spectra of very high energy γ -ray sources*, *PhRvD* **98** (2018) 041302 [1808.07596].

[15] C. Steppa and K. Egberts, *Modelling the galactic very-high-energy γ-ray source population*, *A&A* **643** (2020) A137.

[16] M. Cataldo, G. Pagliaroli, V. Vecchiotti and F.L. Villante, *The tev gamma-ray luminosity of the milky way and the contribution of h.e.s.s. unresolved sources to very high energy diffuse emission*, *ApJ* **904** (2020) 85.

[17] F. Aharonian, A.G. Akhperjanian, A.R. Bazer-Bachi, M. Beilicke, W. Benbow, D. Berge et al., *Observations of the Crab nebula with HESS*, *A&A* **457** (2006) 899 [astro-ph/0607333].

[18] Astropy Collaboration, T.P. Robitaille, E.J. Tollerud, P. Greenfield, M. Droettboom, E. Bray et al., *Astropy: A community Python package for astronomy*, *A&A* **558** (2013) A33 [1307.6212].

[19] Astropy Collaboration, A.M. Price-Whelan, B.M. Sipőcz, H.M. Günther, P.L. Lim, S.M. Crawford et al., *The Astropy Project: Building an Open-science Project and Status of the v2.0 Core Package*, *AJ* **156** (2018) 123 [1801.02634].